Journal of Luminescence 130 (2010) 1343–1348

Contents lists available at ScienceDirect

Journal of Luminescence

journal homepage: www.elsevier.com/locate/jlumin

Electrospinning preparation and photophysical properties of one-dimensional (1D) composite nanofibers doped with erbium(III) complexes

Xu Sun [a], Bin Li [a,b,*], Luting Song [a], Jian Gong [a], Liming Zhang [b,c]

[a] Key Laboratory of Polyoxometalate Science of Ministry of Education, Department of Chemistry, Northeast Normal University, Changchun 130024, PR China
[b] Key Laboratory of Excited State Processes, Changchun Institute of Optics Fine Mechanics and Physics, Chinese Academy of Sciences, Changchun 130033, PR China
[c] Graduate School of the Chinese Academy of Sciences, Chinese Academy of Sciences, Beijing 100039, PR China

ARTICLE INFO

Article history:
Received 17 July 2008
Received in revised form
31 August 2009
Accepted 15 February 2010
Available online 15 March 2010

Keywords:
Electrospinning
Polymer composite fibers
Erbium(III) complex
Near-infrared photoluminescence

ABSTRACT

1D composite nanofibers of poly(vinylpyrrolidone) (PVP, $M_W \approx 60{,}000$) doped with three Er(III) complexes were prepared by electrospinning. They demonstrated strong near-infrared (NIR) photoluminescence (PL) at 1535 nm and ternary $Er(TTA)_3Phen$ (denoted as Er2, where TTA=2-thenoyltrifluoroacetonate; Phen=1,10-phenanthroline) fibers (Er2/PVP) exhibited maximum PL intensity. The crystal structure of Er2 complex has been determined by X-ray diffraction measurements. Er2 doped in fibers exhibited better thermal stability of NIR PL than the pure Er2 complex. These luminescent composite fibers have potential application in optical amplifiers.

1. Introduction

Erbium-doped materials have attracted considerable attention since erbium-doped fiber amplifiers (EDFAs) appeared in 1987, due to their potential application in the optical amplifiers [1–3]. Er^{3+} ion shows characteristic emission centered at 1535 nm via an intra-4f shell transition from its first excited state ($^4I_{13/2}$) to the ground state ($^4I_{15/2}$), which corresponds to the minimum loss transmission window of quartz fibers in the optical communication network [4]. Great effort is devoted to the erbium(III) organic complexes [5], because the full width at half maximum (FWHM) of any Er-doped inorganic material is relatively small [6]. In the organic complexes, lanthanide ions are chelated with organic ligands. Such lanthanide chelates can protect the metal ions from vibrational coupling and increase the light absorption cross-section via "antenna effects" [7,8]. Recently, great attention has been paid to the potential materials for fabricating low-cost optical amplifiers, such as Er(III) complex doped sol–gel, mesoporous and polymer materials [4,9,10]. However, the doped amount is low due to poor solubility of Er(III) complex in precursor of gel or mesoporous materials, and it is difficult to obtain continuous super long, flexible and uniform diameter fibers using them as matrices. There is hardly any report on Er^{3+} ions doped 1D nanomaterial [11]. To the best of our knowledge, there is no literature on the preparation of erbium-doped 1D composite nanofibers using electrospinning method.

1D nanostructural materials have drawn extensive interest recently due to their extensive application [12–14]. Electrospinning technique is a simple and low-cost method for making continuous ultrafine nanofibers with diameters ranging from tens of nanometers to several micrometers [15,16], which depends on the solvent and the solution properties [17]. The composite nanofibers processed from solution are mechanically flexible and they combine the advantages of one-dimensional nanostructures, organic and inorganic materials.

In this paper, 1D composite nanofibers containing three Er(III) complexes were prepared through an electrospinning approach, and related photophysical properties were investigated. It is found that the thermal stability of NIR PL is improved by doping Er(III) complex in nanofibers.

2. Experimental

2.1. Materials

PVP was supplied by Beijing Yi Li Chemical Factory. All starting chemicals including 1,1,1,5,5,5-hexafluoro-2,4-pentanedione (HFA), 2-thenoyltrifluoroacetone (HTTA), 1,10-phenanthroline

* Corresponding author at: Key Laboratory of Polyoxometalate Science of Ministry of Education, Department of Chemistry, Northeast Normal University, Changchun 130024, PR China. Tel./fax: +86431 86176935.
E-mail address: lib020@yahoo.cn (B. Li).

0022-2313/$ - see front matter © 2010 Elsevier B.V. All rights reserved.
doi:10.1016/j.jlumin.2010.02.024

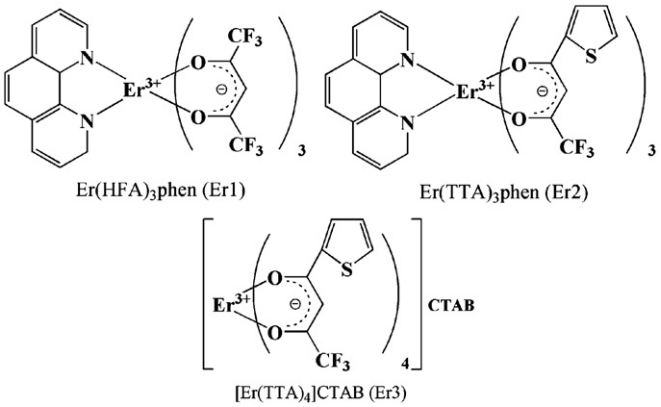

Fig. 1. Chemical structures of Er(III) complexes.

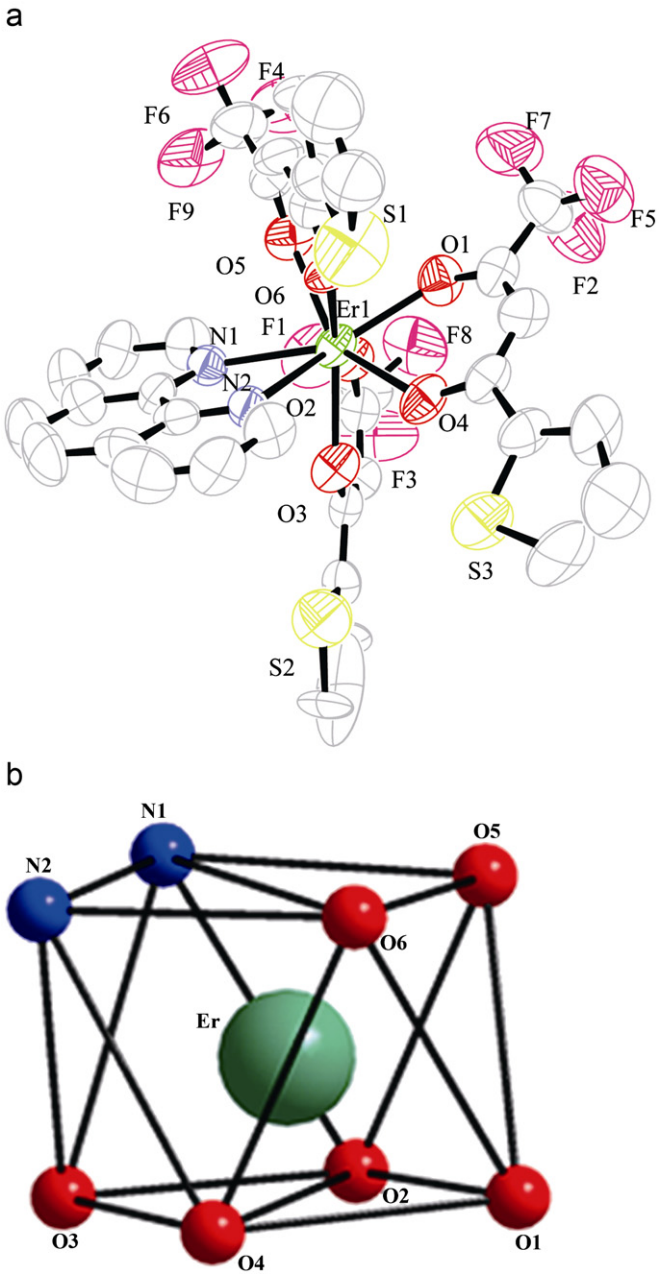

Fig. 2. (a) OPTEP plot for Er2 with ellipsoids drawn at the 50% probability level. The C and H atoms were omitted for clarity. (b) Coordination polyhedron of the Er^{3+} ion.

(Phen) and cetyltrimethylammoniumbromide (CTAB) were supplied by Shenyang Guo Yao Chemical Factory. Erbium oxide (Er_2O_3, 99.99%) was supplied by Changchun Institute of Applied Chemistry, Chinese Academy of Sciences. All reagents were analytical grade and used as received. Erbium chloride was obtained by dissolving Er_2O_3 in hydrochloric acid.

2.2. Synthesis of erbium complexes

2.2.1. Synthesis of Er(HFA)$_3$Phen (Er1)

Er1 was synthesized according to the conventional method with some minor modifications [18]. 3 mmol HFA, 1 mmol $ErCl_3 \cdot 6H_2O$ and 1 mmol phen were dissolved in hot ethanol under constant stirring. After cooling, 3 mmol of a 2 mol/L NaOH aqueous solution was added to the resulting solution under constant stirring. Then, the mixture was stirred at 60 °C for 5 h. The crude product was collected by filtration and washed with ethanol. Yield: 80%. IR spectroscopy (KBr pellet): [cm^{-1}] 3058, 3025, 2966, 2928, 1549, 1518,1458 (C=O, chelated to Er^{3+}), 618, 508, 413 (O–Er–O). Anal. Calcd for $C_{27}H_{11}ErF_{18}N_2O_6$: C, 33.48; H, 1.15; N, 2.89; found: C, 33.69; H, 1.41; N, 3.17.

2.2.2. Synthesis of Er(TTA)$_3$Phen (Er2)

The synthetic procedure of Er2 was similar to that of Er1 except that TTA was used instead of HFA. Yield: 75%. IR spectroscopy (KBr pellet): [cm^{-1}] 3046, 3015, 2936, 2948, 1541, 1528, 1468 (C=O, chelated to Er^{3+}), 619, 511, 412 (O–Er–O). Anal. Calcd for $C_{36}H_{20}ErF_9N_2O_6S_3$: C, 42.73; H, 1.98; N, 2.77; found: C, 42.38; H, 2.10; N, 3.12.

2.2.3. Synthesis of Er(TTA)$_4$CTAB (Er3)

Er3 was synthesized according to the conventional method with some minor modification [18]. Under stirring, 1.776 g of HTTA was added to a hot solution of 0.806 g of CTAB in 50 mL of alchhol, after it was dissolved. 10 mL of a 0.77 M NaOH solution and 0.516 g of a $ErCl_3$ alcohol solution were dropped into the solution. The mixture was refluxed for 1 h. Then cooled, filtered, and recrystallized in alcohol, and then dried over P_2O_5. Yield: 70%. IR spectroscopy (KBr pellet): [cm^{-1}] 3100, 3015, 2966, 2928, 1549, 1518,and 1458 (C=O, chelated to Er^{3+}), 618, 508, and 413

Table 1
Crystal data and structure refinement for Er2.

Empirical formula	C_{36} H_{20} Er F_9 N_2 O_6 S_3
Formula weight	1010.98
Temperature (K)	293(2)
Wavelength (Å)	0.71073
Crystal system	Triclinic
Space group	P-1
Unit cell dimensions	a=9.796(7) Å; α=92.941(12)°
	b=13.101(9) Å; β=92.248(12)°
	c=15.466(11) Å; γ=102.486(11)°
Volume (Å^3)	1933(2)
Z	2
Calculated density (Mg/m^3)	1.737
Absorption coefficient (mm^{-1})	2.423
F(0 0 0)	990
Crystal size (mm^3)	0.15 × 0.14 × 0.12
θ range for data collection (deg°)	1.32 to 25.99
Limiting indices	$-12 \le h \le 9$, $-16 \le k \le 16$, $-14 \le 1 \le 18$
Reflections collected/Unique	10619 / 7326 [R_{int}=0.0440]
Completeness to θ = 25.99° (%)	96.8
Data/restraints/parameters	7326/0/494
Goodness-of-fit on F^2	0.974
Final R indices [$I > 2$ sigma(I)]	$R1$=0.0827, $wR2$=0.1756
R indices (all data)	$R1$=0.1434, $wR2$=0.1998
Largest diff. peak and hole/ e Å^{-3}	1.774 and −0.801

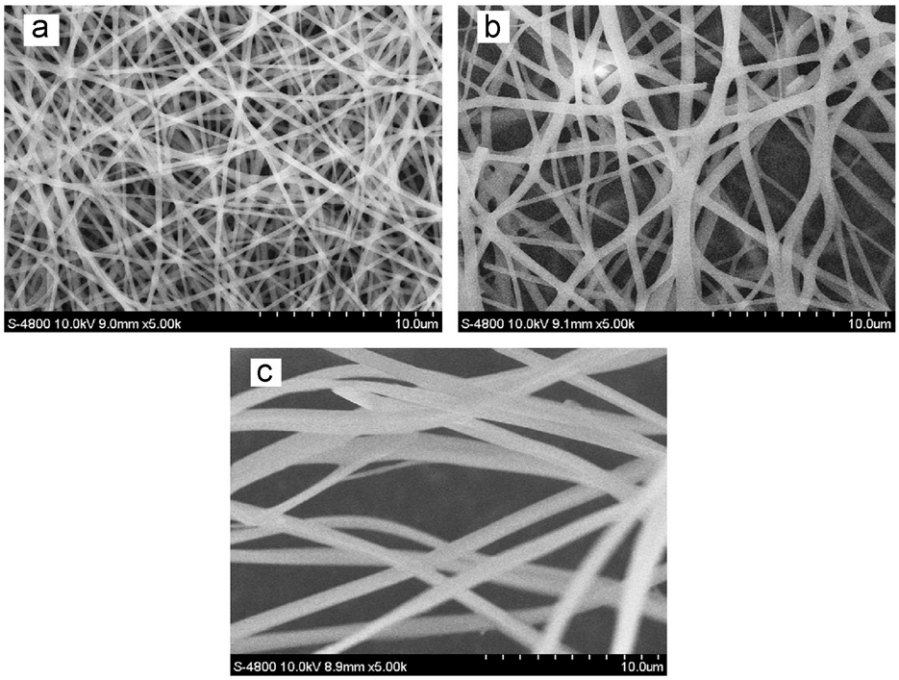

Fig. 3. SEM images of Er/PVP fibers: (a) Er1/PVP, (b) Er2/PVP, and (c) Er3/PVP.

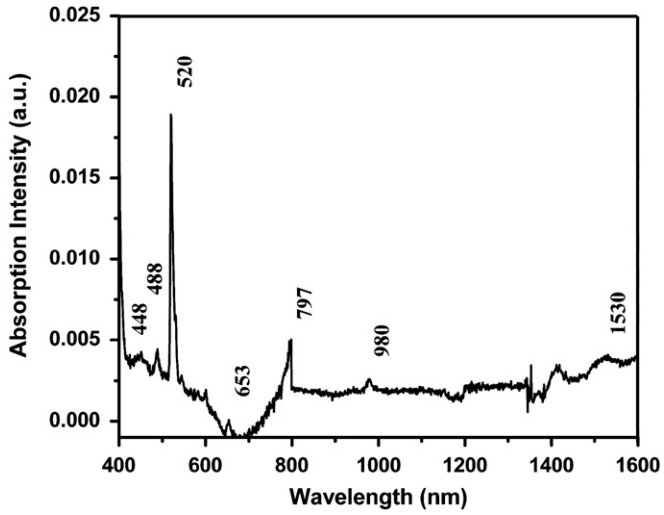

Fig. 4. UV–vis–NIR absorption spectrum of Er2 dissolved in acetone at room temperature (1×10^{-5} mol/L).

(O–Er–O). Anal. Calcd for $C_{51}H_{62}ErF_{12}NO_8S_4$: C, 45.83; H, 4.38; N, 1.05; found: C, 46.02; H, 4.07; N, 1.24.

Chemical structures of Er complexes are depicted in Fig. 1.

2.3. Preparation of composite fibers doped with Er(III) complexes

In the preparation, PVP was dissolved in dichloromethane solvent to prepare a 25 wt% solution. Then a controlled amount of Er1, Er2, and Er3 was added, into 25 wt% PVP solutions with magnetic stirring at room temperature for 12 h to ensure uniform mixing. To improve solubility of the Er(III) complexes in dichloromethane, a small amount of dimethylformamide (DMF) was added until Er(III) complexes dissolved completely. The electrospinning solution was loaded into a glass syringe equipped with a spinneret. The spinneret was connected to a high-voltage power supply. A piece of aluminum foil was used to wrap a

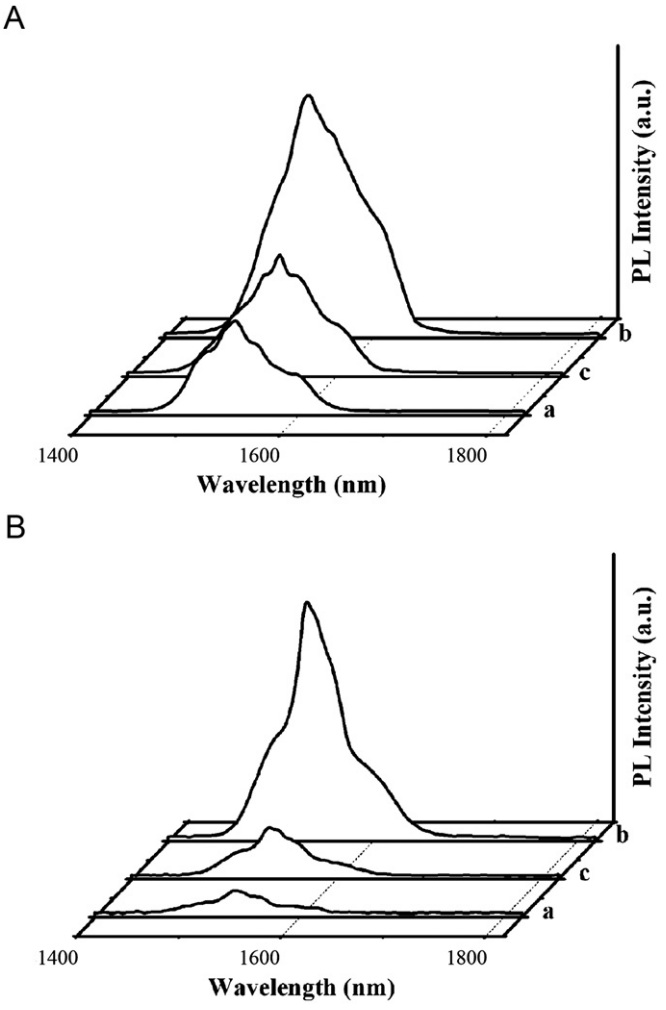

Fig. 5. NIR PL spectra excited at 488 nm at room temperature. (A) Er complexes: (a) Er1, (b) Er2, (c) Er3 and (B) Er/PVP fibers: (a) Er1/PVP, (b) Er2/PVP, (c) Er3/PVP.

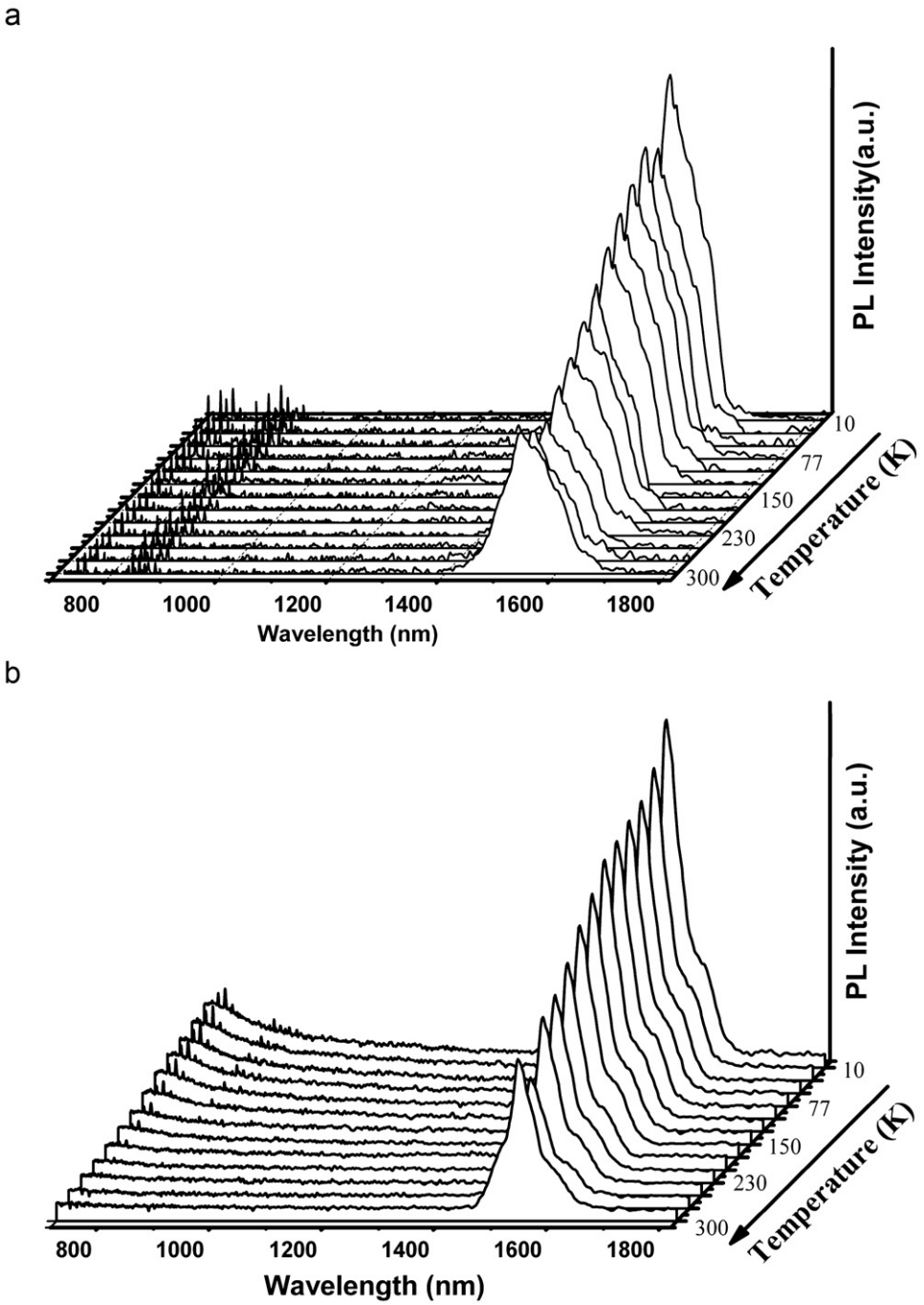

Fig. 6. Emission spectra for (a) Er2 and (b) Er2/PVP fibers at various temperatures under 488 nm excitation.

collector plate that serves as an electrode to collect these nanofibers. A 18 kV accelerating voltage and a 25 cm working distance between the spinneret and the collector plate were used to carry out the electrospinning process [19]. The corresponding concentration was 1.18×10^{19} Er(III) cm^{-3}, which indicated that Er(III) complex number in per cubic centimeter 25 wt% PVP solution is 1.18×10^{19} Er^{3+}.

2.4. Measurements

Data for Er2 Complex were collected on a Siemens Smart CCD diffractometer with Mo K_α monochromatic radiation (λ=0.71073 Å) at room temperature. The linear absorption coefficients, scattering factors for the atoms, and the anomalous dispersion corrections were taken from International Tables for X-ray Crystallography. Empirical absorption corrections were applied. The structures were solved by the direct method and refined by the full-matrix least-squares method on F^2 using the SHELXL97 crystallographic software package. Anisotropic thermal parameters were used to refine all non-hydrogen atoms except for N_1 and N_2. The hydrogen atoms for TTA and phen were fixed in ideal position and the non-hydrogen atoms were refined anisotropically.

The single-crystal X-ray diffraction data for Er2 complex were recorded on a Siemens Smart CCD diffractometer with Mo K_α monochromatic radiation (λ=0.71073 Å). The size and morphology of the composite fibers were observed with a Hitachi S-4800 scanning electron microscope (Aitachi) (SEM). Fourier-transform

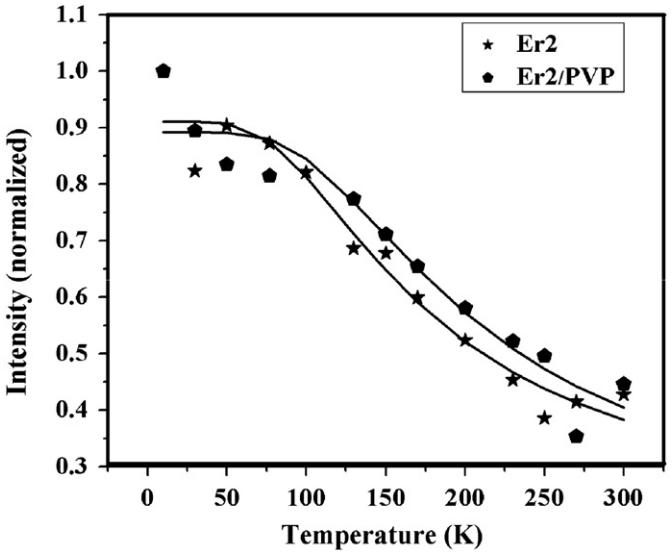

Fig. 7. Temperature dependence of emission intensities of the $^4I13/2 \rightarrow {}^4I_{15/2}$ transition on temperature.

infrared (FTIR) spectra were measured from 4000 to 400 cm^{-1} on an FTS135 infrared spectrophotometer (BIO-RAD). The UV–vis–NIR spectra were recorded by a Cary 500 scan spectrophotometer (VARIAN). The NIR PL spectra were taken with a PL9000 equipment (BIO-RAD).

3. Results and discussion

3.1. Crystal structure of the Er2 complex

For Er2, the molecular structure with the numbering scheme and the color representation of the core atoms are given in Fig. 2. Key experimental parameters of the complex structure are given in Table 1. The single crystal X-ray structure analysis revealed that the central Er^{3+} is coordinated by six oxygen atoms from three TTA ligands with Er–O bond lengths ranging from 2.288 to 2.315 Å and two nitrogen atoms from a phen ligand with Er–N bond lengths of 2.525 and 2.556 Å, adopting a square antiprism coordination environment (Fig. 2b). In the β-diketone rings, the average bond lengths of C–C and C–O are 1.395 and 1.261 Å, respectively, between the typical single– and double– bond distances. It can be explained in terms of conjugation between the thienyl ring and the coordinated β-diketone, which results in electron delocalization within this moiety [20].

3.2. Fiber morphology

Fig. 3 shows the SEM images of composite fibers. It can be seen that the fibers with length of several millimeters have smooth surface and uniform distribution in diameter. The average diameters for samples *a*, *b* and *c* are about 250, 650 and 800 nm, respectively. Addition of DMF should be responsible for the difference in size.

3.3. UV–vis–NIR absorption spectra

Fig. 4 shows the UV–vis–NIR absorption of Er2 dissolved in acetone (1×10^{-5} mol/L) at room temperature. The spectrum consists of 7 absorption bands, corresponding to the transitions from the ground state $^4I_{15/2}$ to the excited states, i.e. $^4F_{5/2}$(448 nm), $^4F_{7/2}$(488 nm), $^2H_{11/2}$(520 nm), $^4F_{9/2}$(653 nm), $^4I_{9/2}$(797 nm), $^4I_{11/2}$(980 nm), and $^4I_{13/2}$(1530 nm).

3.4. NIR PL properties

Fig. 5(a) displays PL spectra of erbium complexes excited at 488 nm by an Ar^+ laser at room temperature. The broad emission bands of Er1, Er2 and Er3 are centered at 1538, 1538, and 1545 nm, respectively, which are attributed to the $^4I_{13/2}$ to $^4I_{15/2}$ transition [21]. The FWHM is as wide as 80–100 nm, which is of significance for optical amplification. Under the same excitation density, Er2 exhibits the maximum PL intensity, and Er1 exhibits the minimum at 1538 nm. This may be the due to the mismatch of energy between the resonance level of the Er^{3+} ion and the triplet state of the HFA ligand. For Er2 and Er3, the TTA ligand can remarkably enhance the luminescence intensity. A possible reason may be conjugation structure between the thienyl ring and the coordinated β-diketone resulting in the delocalization of electron density of the coordinated β-diketone chelate ring. It is obvious that TTA ligand sensitizes Er^{3+} ions efficiently and provides an optimal condition for radiative decay. From Fig. 5(b), the PL enhancement was found to be in an order of the relative emission intensity of composite fibers: I(Er2/PVP) > I(Er3/PVP) > I(Er1/PVP). No change in branch ratio is observed, suggesting similar sensitization process and coordination geometry of Er^{3+} ion in different complexes.

To compare the thermal stability of NIR PL of pure Er complex and Er complex in PVP fibers, temperature dependence of NIR PL intensity of Er2 and Er2/PVP fibers is measured under 488 nm excitation and in a temperature range of 10–300 K. The emission spectra of Er2 complex and the Er2/PVP fibers at different temperatures are shown in Fig. 6, and the temperature dependence of the integral NIR PL intensities of the $^4I_{13/2} \rightarrow {}^4I_{15/2}$ transition are shown in Fig. 7. From Fig. 7, it is found that the variation of the emission intensity for the Er^{3+} ions in the composite fiber shows a remarkable difference related to that in the pure complex. The PL intensities of Er2 complex and Er2/PVP fibers decrease slowly at first with increase in temperature, suggesting the emission intensity is appropriate to saturate, since quenching effects are diminished with decrease in temperature. The non-radiative decay is mainly induced by temperature effect, i.e. thermal quenching. The emission intensities of Er2 complex and Er2/PVP fibers decrease monotonically with increase in temperature in the 100–300 K range.

The temperature dependence of the integrated PL intensity can be expressed by the thermal activation equation [22,23]

$$I(T) = I_0/(1 + \alpha \exp(-E_A/K_B T))$$

where E_A is the activation energy of the thermal quenching process, K_B is Boltzmann's constant, α is the proportional coefficient, I_0 is the emission intensity at 0 K, and T is the absolute temperature. By fitting our experimental data using the above Equation, the values of E_A in pure complex Er2 and Er2/PVP composite fibers are estimated to be 31.55 and 37.51 meV, respectively. The improved value of E_A indicates that the temperature stability of PL of the composite fibers is better than that of the pure complex. The PVP matrix restricts the vibrations of the ligands, resulting in a decrease of the non-radiative transition caused by ligands vibrations, resulting in improvement of thermal stability of NIR PL of Er(III) complex.

4. Conclusions

We prepared uniform composite fibers containing three erbium complexes with 1535 nm strong NIR PL by

electrospinning and demonstrated the crystal structure of the Er2 complex. The diameters of the composite fibers were generally measured in the range of 250–800 nm. The optical properties of the composite fibers are investigated and compared with those of the pure Er(III) complexes. The temperature stability of the PL intensity of the composite fibers is improved in comparison with that of the pure complex. These results indicate that the Er/PVP composite fiber is a promising candidate for optical amplifiers.

Acknowledgment

The authors thank the National Natural Science Foundation of China (Grant no. 50872130).

Appendix A. Supplementary material

Supplementary data associated with this article can be found in the online version at doi:10.1016/j.jlumin.2010.02.024.

References

[1] O.H. Park, S.Y. Seo, B.S. Bae, J.H. Shin, Appl. Phys. Lett. 82 (2003) 2787.
[2] G.A. Kumar, R.E. Riman, Chem. Mater. 17 (2005) 5130.
[3] Q. Wang, N.K. Dutta, R. Ahrens, J. Appl. Phys. 95 (2004) 4025.
[4] H. Wang, G. Qian, Z. Wang, J. Zhang, Y. Luo, M. Wang, J. Lumin. 113 (2005) 214.
[5] K. Kuriki, Y. Koike, Y. Okamoto, Chem. Rev. 102 (2002) 2347.
[6] J. Barbillat, P. Le Barny, L. Divay, E. Lallier, A. Grisard, R. Van Deun, P. Fias, Rev. Sci. Instrum. 74 (2003) 4954.
[7] S. Sato, M. wada, Bull. Chem. Soc. Jpn. 43 (1970) 1955.
[8] S. Moynihan, R. Van Deun, K. Binnemans, G. Redmond, Opt. Mater. 29 (2007) 1821.
[9] L.N. Sun, H.J. Zhang, C.Y. Peng, J.B. Yu, Q.G. Meng, L.S. Fu, F.Y. liu, X.M. Guo, J. Phys. Chem. B 110 (2006) 7249.
[10] D. Zhang, C. Chen, X. Sun, Y.G. Zhang, X.Z. Zhang, A. Wu, B. Li, D. Zhang, Opt. Commun. 278 (2007) 90.
[11] Z. Wang, J.L. Coffer, Nano Lett. 2 (2002) 1303.
[12] I. Gorelikov, E. Kumacheva, Chem. Mater. 16 (2004) 4122.
[13] J. Aldana, N. Lavelle, Y. Wang, X. Peng, J. Am. Chem. Soc. 127 (2005) 2496.
[14] E. Yan, Z. Huang, Y. Xin, Q. Zhao, W. Zhang, Mater. Lett. 60 (2006) 2969.
[15] Y. Dror, W. Salalha, R.L. Khalfin, Y. Cohen, A.L. Yarin, E. Zussman, Langmuir 19 (2003) 7012.
[16] Q. Zhao, Z. Huang, C. Wang, Q. Zhao, H. Sun, D. Wang, Mater. Lett. 61 (2007) 2159.
[17] J.M. Deitzel, J. Kleinmeyer, D. Harris, N.C.B. Tan, Polymer 42 (2001) 261.
[18] L.R. Melby, N.J. Rose, E. Abramson, J.C. Caris, J. Am. Chem. Soc. 86 (1964) 5117.
[19] H. Yu, H. Song, G. Pan, S. Li, Z. Liu, X. Bai, T. Wang, S. Lu, H. Zhao, J. Lumin. 124 (2007) 39.
[20] J.B. Yu, H.J. Zhang, L.S. Fu, R.P. Deng, L. Zhou, H.R. Li, F.Y. Liu, H.L. Fu, Inorg. Chem. Commun. 6 (2003) 852.
[21] L.N. Sun, H.J. Zhang, L.S. Fu, F.Y. Liu, Q.G. Meng, C.Y. Peng, J.B. Yu, Adv. Funct. Mater. 15 (2005) 1041.
[22] H. Zhang, H. Song, H. Yu, X. Bai, S. Li, G. Pan, Q. Dai, W. Li, S. Lu, X. Ren, H. Zhao, J. Phys. Chem. C 111 (2007) 6524.
[23] D.S. Jiang, H. Jung, K. Ploog, J. Appl. Phys. 64 (1988) 1371.